Contents

1. INTRODUCTION 1

2. DESIGN REQUIREMENTS FOR THE LOW-LEVEL CALIBRATION SYSTEM 2
2.1 The Measurement Problem 2
2.2 Calibration System: Performance Requirements 2
2.3 Transfer-Standard Definitions 3

3. DESCRIPTION OF THE 1.06 μm CALIBRATION SYSTEM 4
3.1. Laser Source and Shutter 5
3.2 Beam Steering and Polarizing Optics 5
3.3 Collimating Optics and Modulator 5
3.4 Multiple-Reflection Beamsplitter/Attenuator 6
3.5 Laboratory Reference Standard 8
3.6 Waveform-measuring Instrument: Oscilloscope 9

4. CALIBRATION OF LASER RADIOMETERS FOR PULSE-ENERGY RESPONSE 9

5. CALIBRATION OF LASER RADIOMETERS FOR PEAK-POWER RESPONSE 11
5.1 Peak-power Calibration 11
5.2 Bandwidth of Peak-Power Transfer Standards 13

6. MEASUREMENT OF DETECTOR IMPULSE RESPONSE 13
6.1 Impulse Laser 13
6.2 Measurement of Detector Impulse Response 14

7. MEASUREMENT UNCERTAINTY 16
7.1 Uncertainty in the Laboratory Reference Standard 17
7.2 Pulsed-Laser Low-Level Measurement System Uncertainty 17
7.3 Pulsed-Laser Radiometer Uncertainty Components 21

8. MEASUREMENT ASSURANCE 22
8.1 Calibration History of the Laboratory Reference Standard 22
8.2 Laser Beamsplitter Ratio Measurements 23
8.3 Using the Calibration History of Check Standards to Monitor the Low-Level System 24
8.3.1 Check Standards for Pulse-Energy Calibrations 24
8.3.2 Check Standards for Peak-Power Calibrations 24
8.4 Revising the Uncertainty Levels from Accumulated Data 26

9. FUTURE CHANGES IN CALIBRATION SYSTEM 26

10. REFERENCES 27

Appendix A: Sample Calibration Report 28

APPENDIX B. Calibration Procedure Outline 35

APPENDIX C. Impulse Response Measurement and Bandwidth Correction Calculation 36
C.1 The need for impulse response measurement of pulsed-laser detectors 36
C.2 Bandwidth correction procedure 37

APPENDIX D: Suitable Transfer Standards and Shipping Instructions 38
D.1. Transfer standards that are suitable for calibration 38
D.2. Shipping instructions for transfer standards 38

Calibration Service for Low-level Pulsed-Laser Radiometers at 1.06 μm: Pulse Energy and Peak Power

Rodney W. Leonhardt
National Institute of Standards and Technology
Boulder, Colorado 80305

I describe the calibration service provided by the National Institute of Standards and Technology (NIST) for peak power or pulse energy of low-level laser pulses at the wavelength of 1.06 μm. This service supports the calibration of pulsed-laser radiometers at peak power levels of 40 nW to 5 mW and pulse energy from 100 fJ to 10 nJ. Laser-pulse durations can be varied from 20 ns to 2 μs depending on the instrument to be calibrated and laboratory reference-standard requirements. Typical expanded uncertainties range from 6 to 8 %.

KEY WORDS: beamsplitter attenuator; impulse response; low-level 1.06 μm laser measurements; peak power; pulse energy

1. INTRODUCTION

This service primarily supports the military services and their contractors with the calibration of pulse-energy and peak-power laser radiometers at a wavelength of 1.06 μm. Typically, these radiometers are transfer standards, which are then used to calibrate systems supporting laser rangefinders and guidance receivers. The calibrated radiometers provide traceability to the national standard C-series calorimeters developed and operated by NIST.

Design requirements for the calibration system and for pulsed-laser radiometers will be reviewed in this document. A complete description of the optical system and specific calibration procedures are included. Calibration uncertainties and measurement assurance procedures are discussed in detail.

The basic measurement system (Section 3) consists of a laser source, collimating optics, modulator, beamsplitter, laboratory reference-standard, and oscilloscope. The oscilloscope is used to record the voltage waveform output from the instrument under test (IUT) while the system measures the peak power or pulse energy of the laser signal. The relationship between the voltage waveform and the laser pulse characteristics yields calibration factors for pulse energy (joules/volt) or peak power (volts/watt). Other calibration factors could be used.

The dynamic range of the low-level measurement system is 40 nW to 5 mW for peak-power, and 100 fJ to 10 nJ for laser-pulse energy. However, it should be noted that not all pulse energies or peak powers are continuously achievable throughout the stated range. There is a substantial amount of flexibility in tuning the levels of the measurement system, but the discrete nature of the beamsplitter (Section 3.4) and the requirements of the reference-standard (Section 3.5) ultimately limit this capability.

2. DESIGN REQUIREMENTS FOR THE LOW-LEVEL CALIBRATION SYSTEM

2.1 The Measurement Problem

The design and calibration of transfer standards suitable for the measurement of low-level, short-duration laser pulses present sensitivity and speed requirements for a detector that can usually be met only with semiconductor devices. A laser power or energy meter using such a detector will give a measurable response V(t), usually electrical, as a result of absorbing some portion of the incident laser beam [1].

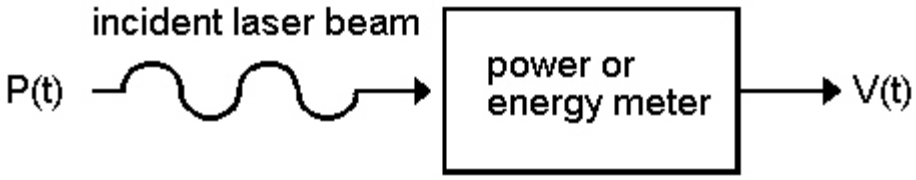

Figure 1. Conversion of laser pulse to voltage signal.

Previous work at NIST [1] has shown that if the transfer detector is linear and time invariant, then

$$\int_0^\infty V(t)dt = KE, \qquad (1)$$

where *V(t)* is the response of the detector to the laser pulse *P(t)*, *K* is the calibration constant in V/W, and *E* is the energy in the laser pulse. Accordingly, the measurement system must be able to generate laser pulses to characterize and calibrate the *K* response of these transfer standards.

2.2 Calibration System: Performance Requirements

A system that can calibrate the responsivity of transfer standards useful for laser receivers or rangefinders must be able to generate very low levels of pulsed-laser radiation spanning five orders of magnitude in power. The laser pulses need to be fairly narrow in duration, extending from about 20 to 500 ns in duration for peak-power calibrations, and 20 ns to 2 μs for pulse-energy calibrations. Pulse repetition rates from 50 Hz to 300 kHz are required by the different transfer-standard designs. Sufficient laser energy must be generated such that the laboratory reference standard can make measurements to provide a calibration traceability to higher-accuracy primary standards. For peak-power measurements, an instrument that can accurately measure the peak voltage of a 20 ns waveform is also necessary. The desired expanded uncertainty for transfer-standard calibrations is no greater than 10 %, with a goal of 5 % in the future.

2.3 Transfer-Standard Definitions

In order to minimize confusion, I will define the types of laser measurement standards referred to in this document. Primary standards or national standards are instruments developed at NIST to provide measurement traceability from laser power or energy to higher-accuracy electrical standards. A laboratory reference standard or secondary transfer standard is a device that is calibrated against a primary standard, and then used in a secondary calibration system to serve as the standard. A field transfer standard is an instrument that is calibrated against the laboratory standard, and is used at remote locations away from the NIST site to continue the calibration chain. For the purposes of this document, field transfer standards are pulsed-laser radiometers whose response is calibrated in terms of irradiance or fluence.

Each type of standard has specific performance requirements that make it useful for a particular application. The primary standards emphasize accuracy and low uncertainty at the sacrifice of speed and convenience. The laboratory reference standard must be able to provide traceability between the primary standard and the low-level requirements of the field instruments. The field transfer standards feature sensitivity, speed, and rugged operation, but are not as accurate. Low-level instruments are based on semiconductor detectors in order to provide the sensitivity and portability necessary for an effective field transfer standard.

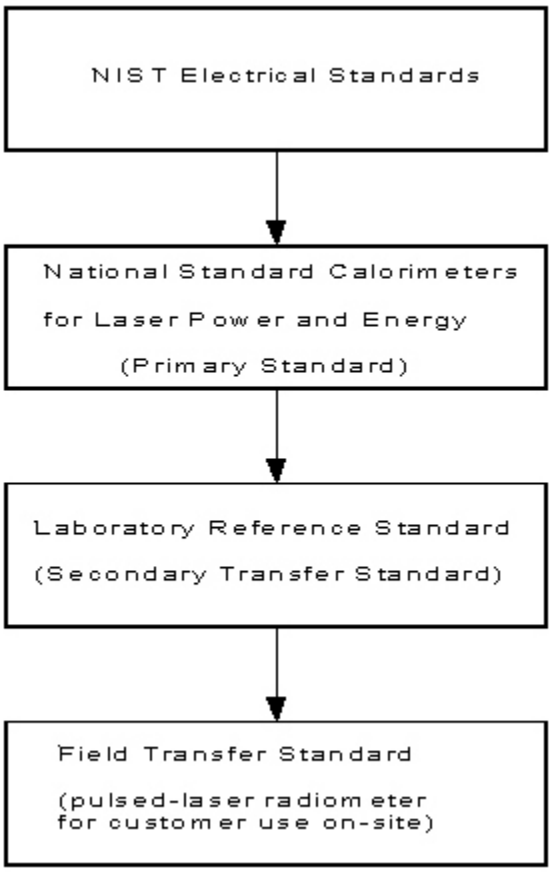

3. DESCRIPTION OF THE 1.06 µm CALIBRATION SYSTEM

The NIST measuring system generates low levels of known peak power and energy to calibrate laser radiometer response. Peak power or energy in any one beam is determined from the known splitting ratios of a precision beamsplitter [2]. A simplified diagram of the calibration system is shown in Figure 3. The principal subsystems of the calibration set-up are:

A. Source laser: diode-pumped Nd:YAG laser

B. Beam-steering and polarizing optics

C. Collimating lenses and modulator

D. Multiple-reflection beamsplitter/attenuator

E. Laboratory reference standard

F. Waveform measuring instrument: oscilloscope

All the instruments shown in Figure 3, except the oscilloscope, are contained in an acrylic-resin enclosure. The enclosure is not airtight, but does block air currents from blowing directly on the reference standard and other equipment. The enclosure is opaque to visible and near-IR light, and serves to keep ambient light from interfering with the very sensitive semiconductor detectors. Safety is enhanced by blocking the scattered light with the opaque panels and containing the laser radiation within a restricted area.

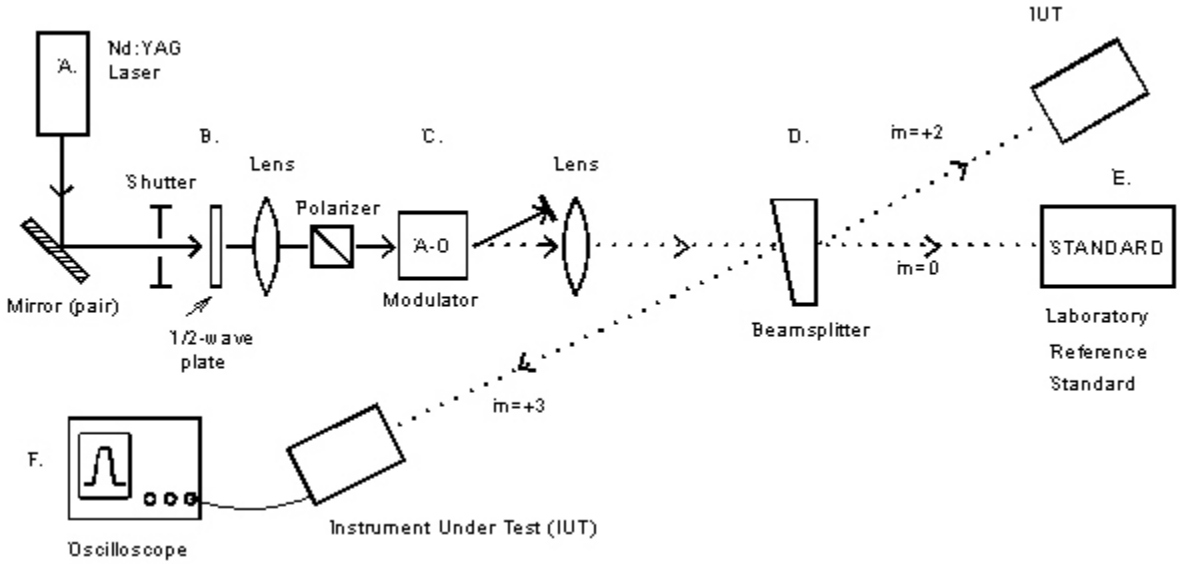

Figure 3. System for calibrating laser pulse energy or peak power at 1.06 µm. Dashed line represents first-order diffracted beam, which has been modulated into pulses.

3.1 Laser Source and Shutter

The source for 1.06 μm radiation is a diode-pumped, solid-state Nd:YAG laser. The laser's center wavelength is 1.0643 ± 0.0002 μm, with spectral width (FWHM) of 0.001 μm. Also, there is output in a lasing mode centered at 1.0617 ± 0.0002 μm with a width (FWHM) of 0.0004 μm. This side mode is 10 dB down from the main power mode and has little effect on the calibration factors.

The laser's output can be controlled between 150 to 1000 mW and still maintain stable operation in a TEM_{oo} mode with a $1/e^2$ diameter of 1 mm at the output window. The laser is linearly polarized with a vertical orientation of the electric field. A mechanical shutter controls the injection of laser power into the measurement system. During a calibration run, this shutter is operated by the computerized data-acquisition system.

3.2 Beam Steering and Polarizing Optics

Dielectric mirrors are used to direct the beam from the laser to the required position and provide precise adjustment for steering it down the optical axis of the calibration system. Polarization control is accomplished with a half-wave plate followed by a polarizing prism. Reflection from the beam steering mirror pair changes the polarization to horizontal, so the half-wave plate is used to rotate the orientation to vertical. Propagation through a Glan laser prism provides a linear polarization state of high purity, with extinction ratio greater than 2000 to 1. Beamsplitter ratios can be determined more accurately if the polarization state of the light is well known, as will be shown in Section 3.4.

3.3 Collimating Optics and Modulator

Divergence of the laser beam is controlled with two lenses that can be adjusted to provide varying degrees of collimation. This allows the beam spot size at the IUT to be manipulated from about 3 to 10 mm. The lenses are mounted on a sliding rail system, and changing the separation distance provides control of the spot size.

The collimating lens pair also provides a focused beam waist centered within the small aperture of the modulator. A smaller (<1 mm) beam waist allows improved modulator performance. Faster rise and fall times, along with a greater depth of modulation, are the benefits of a smaller beam diameter. This is valid whether an acousto-optic or electro-optic modulator is used.

Calibrations in the low-level system are done with the acousto-optic modulator (AOM). The advantages are better pulse-to-pulse stability, higher contrast ratio (on-to-off) and easier alignment of the modulator itself. Pulse durations are limited to greater than 120 ns, with 55 ns rise and fall times for the existing AOM.

An electro-optic modulator (EOM) is being considered for use with the calibration system to provide shorter pulse durations. The modulator has rise and fall times on the order of 10 ns, with a narrowest pulse duration of approximately 20 to 25 ns. However, the performance of the EOM has not been fully characterized and it is not yet available for calibration services.

3.4 Multiple-Reflection Beamsplitter/Attenuator

We make extensive use of multiple-reflection wedged beamsplitters for attenuation in calibration systems for laser power or energy. The theory and use of wedged beamsplitters have been well documented [2][3]. The basic purpose for using a beamsplitter is to generate at least two beams with a known ratio of power. The instruments are positioned in a suitable beam, allowing the measurement of laser power or energy by the reference standard to be transferred to the IUT.

There are two principal advantages to using beamsplitters in laser measurements. If both of the two detectors used with the beamsplitter measure total energy, then laser stability is not important since the detectors are monitoring the beam at the same time. Power measurements require a stable laser, but it is a less critical issue when the beamsplitter method, rather than a substitution method is used. Another important advantage is that the beamsplitter extends the dynamic range of the reference calorimeter since the beamsplitter can function as a calibrated attenuator.

A multiple-reflection wedged beamsplitter (Figure 4) is a transparent optical component that has highly polished flat surfaces and is made of a well-characterized material. Given the beamsplitter's index of refraction, wedge angle, and angle of incidence (Table 3.1), Snell's and Fresnel's laws of refraction and reflection can be used to calculate the relative powers of the emerging beams (Table 3.2). In the near-IR wavelength region, fused silica can be used to attenuate the laser and produce the required low levels of pulsed power. Fused silica has been thoroughly studied at various wavelengths, and its dispersion equation is well documented [4].

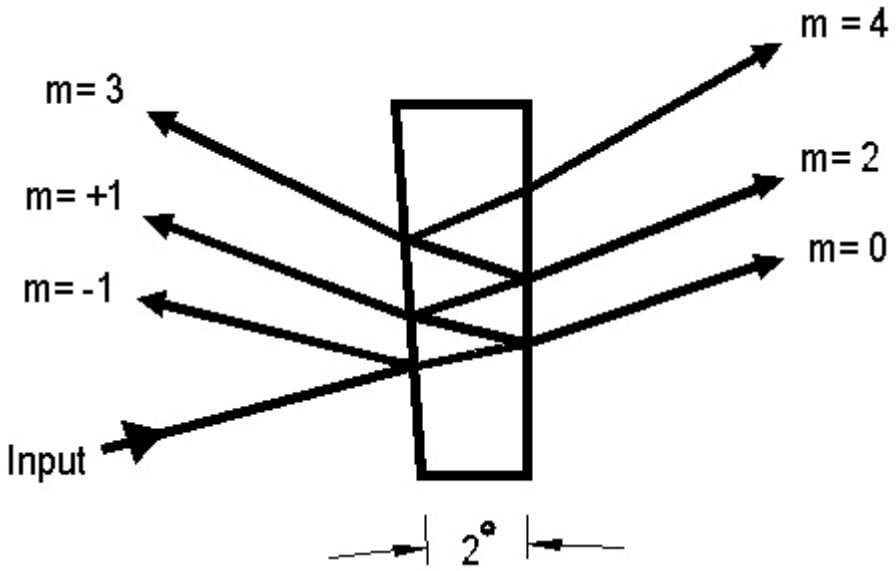

Figure 4. Multiple-reflection wedged beamsplitter.

Table 3.1. Properties of the multiple-reflection beamsplitter.

Material: SiO_2 : fused silica	Index of Refraction: 1.4496 ± 0.0001 [4]
Wedge Angle: 2.0 ± 0.1°	Angle of Incidence: -8.71 ± 0.04°
Wavelength: 1.064 ± 0.003 μm	Index of Refraction of Air: 1.00024 ± 0.00001 [5]

There are two common techniques used to align the beamsplitter in the laser beam and produce a consistent angle of incidence. The beamsplitter can be oriented so that the incident beam bisects the reflected m = – 1 and +1 beams. This orientation provides a small incident angle, but requires long optical path lengths to get the necessary physical separation of the different beams. This alignment is less susceptible to polarization effects than methods with a large angle of incidence.

An alternate method (Figure 5) provides the required beam separation by increasing the angle of incidence. In this method, the transmitted m = +2 beam is reflected back on itself and through a small hole in a card. The beamsplitter is then rotated until the m = +2 retroreflection is concentric with the m = +3 beam. When this condition is achieved with a 1.06 μm wavelength laser beam, then the angle of incidence is approximately 8.71°. The low-level calibration system uses this method of alignment.

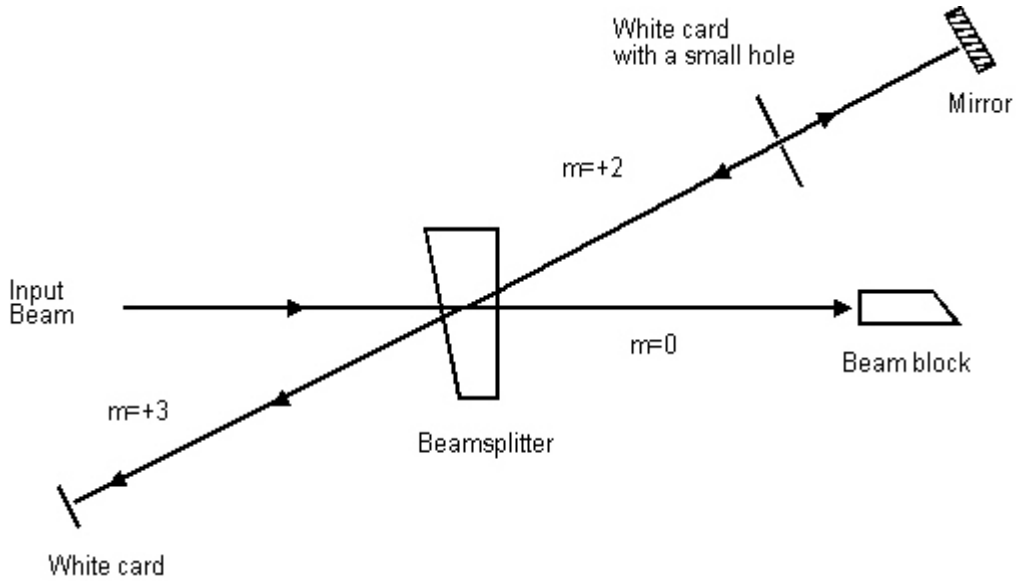

Figure 5. Retroreflection alignment method used for the low-level calibration system.

Table 3.2. Fused-silica beamsplitter ratios calculated from attributes listed in Table 3.1.

Beam A (order, m=)	Beam B (order, m=)	Ratio A/B vertical polarization	Ratio A/B horizontal polarization	Ratio A/B mixed (50 %) polarization	Difference of V & H polarization (%)
0	+1	29.28 ± 0.15	30.15 ± 0.15	29.72 ± 0.15	2.92
0	+2	867 ± 4	899 ± 4	883 ± 4	3.65
0	+3	25771 ± 129	26722 ± 134	26246 ± 131	3.62
+1	+2	29.61 ± 0.15	29.82 ± 0.15	29.72 ± 0.15	0.73
+2	+3	29.72 ± 0.15	29.71 ± 0.15	29.72 ± 0.15	0.02

3.5 Laboratory Reference Standard

The laboratory reference standard (TC-24) is a calorimetric device that provides traceability for the low-level calibration system. Currently, this instrument is calibrated with the C-series calorimeters, which are laser energy standards designed and operated by the Optoelectronics Division. The C-series calorimeters are primary standards that use electrical substitution heating to provide a traceable link between laser energy and electrical standards at NIST.

TC-24 measures laser energy by using thermocouples to sense the temperature difference between a reference plate and a glass plate that absorbs the laser input. A laser beam is injected for a prescribed period, and electronic circuitry integrates the voltage output of the thermopile. The result is a measurement of the total injected laser-energy. This energy value is converted to average pulse energy or peak power by evaluating other characteristics of the laser pulse during the injection period. Specific measurement techniques and calculations are discussed in Sections 4 and 5.

Since TC-24 is a thermal device it is relatively slow (time constant >10 s), and requires almost five minutes for a single measurement to execute. A baseline measurement is taken before and after a laser injection, so a complete calibration run takes about 15 minutes. The baseline measurements are averaged, and serve to subtract out background light as well as to compensate for the thermal drift in the environment.

The laboratory reference standard has been characterized by measurements comparing it to the C-series primary standards for typical laser power levels at which TC-24 is used. Stability has been an advantage of TC-24, as the traceability with the C-series calorimeters have been very consistent over the last several years with a standard deviation in the calibration factor of less than 0.5 %, as shown in Section 8.1. Another benefit is the ability of TC-24 to be used as the reference standard for both pulse-energy and peak-power calibrations.

3.6 Waveform-Measuring Instrument: Oscilloscope

The pulsed-energy and peak-power radiometers are semiconductor-based and are calibrated such that the peak voltage output corresponds to laser peak power or pulse energy. The voltage measurement is made with a fast (≥400 MHz bandwidth) digitizing oscilloscope. Capabilities of the oscilloscope include waveform-averaging and peak-detection, which reduce the effects of noise when making these measurements at their lowest possible level.

4. CALIBRATION OF LASER RADIOMETERS FOR PULSE-ENERGY RESPONSE

All of the field transfer-standards that measure pulse-energy and are calibrated with this low-level system have been designed and constructed at NIST. These instruments use a silicon PIN photodiode or an APD (avalanche photodiode) for light detection. Both types of photodiodes are commercially available and the APD modules have temperature and bias-compensation circuitry included. The resulting photocurrent is converted to a voltage pulse, and integrated with an electronic amplifier. A calibration is accomplished by relating the peak voltage (or peak-to-peak) output with the energy contained in the laser pulse.

We measure the relationship between the peak output voltage and the laser-pulse energy as follows. A train of laser pulses is generated by passing a continuous-wave (cw) beam through the amplitude modulator. The modulated beam is attenuated by the beamsplitter, with the high-level beam propagating to the laboratory reference standard, and a low-level beam incident onto the IUT (Figure 2). In this case the IUT is a pulse-energy radiometer, and the laboratory standard is TC-24.

Because TC-24 is a relatively slow thermal device (time constant >10 s) it cannot distinguish the individual pulses, but measures the total energy received from the modulated laser beam. By measuring the pulse repetition rate and the laser injection period, and using the attenuation ratio of the beamsplitter, the average pulse-energy incident on the IUT can be calculated. The calibration factor is the incident energy divided by the average peak-voltage output of the radiometer and is reported in joulse/volt. If the radiometer's aperture area is included, the responsivity has units of $(J/cm^2)/V$.

$$K_e = \frac{(MR - B)}{(TC \times BSR \times F \times TP \times PV)}, \qquad \textbf{(2)}$$

where: K_e = pulsed-energy calibration factor (J/V)
MR = laboratory-standard reading
B = average baseline reading by laboratory standard
TC = laboratory-standard-traceable calibration factor (meter reading/J)
BSR = beamsplitter attenuation ratio (A/B ratio from Table 3.2)
F = average pulse-repetition rate (s^{-1})
TP = laser injection-time period (s)
PV = average peak voltage (V)

It should be noted that the integrating amplifier in the radiometer not only integrates the voltage pulse, but also differentiates, resulting in a bipolar signal from the radiometer (Figure 6). Any dc offset from the amplifier will introduce an error when measuring the positive peak, so the user must determine whether there is significant offset before proceeding with a calibration. A dc offset can be corrected by using an ac-coupled oscilloscope if the signal is not further modified by the capacitively coupled input. In the latest version of a pulse-energy radiometer we have avoided this potential problem by using dc coupling and calibrating the signal for peak-to-peak voltage (V^+- V^-).

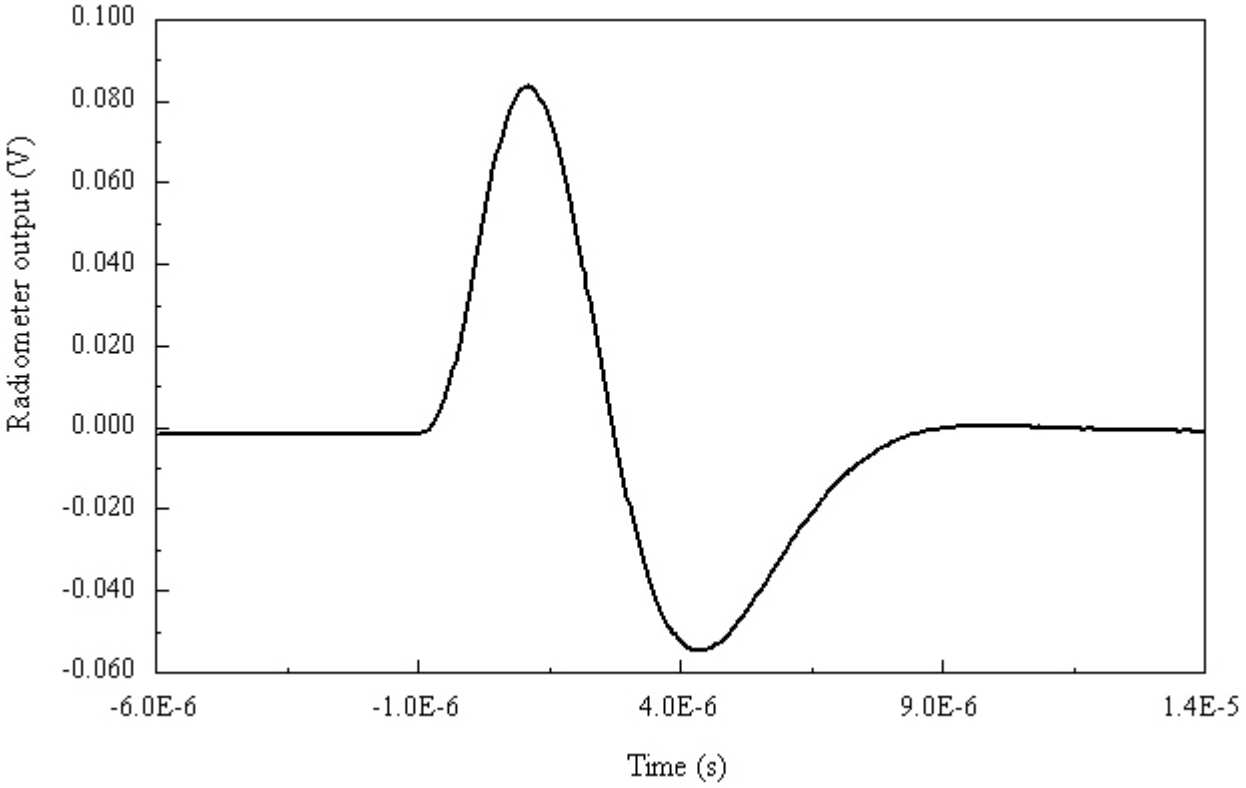

Figure 6. Typical bipolar waveform for pulse-energy calibration.

5. CALIBRATION OF LASER RADIOMETERS FOR PEAK-POWER RESPONSE

5.1 Peak-Power Calibration

Calibration of the peak-power response of laser radiometers is accomplished by correlating a continuous-wave laser signal to a pulsed-signal of equivalent magnitude. The crucial link is a modulation technique that is fast enough to produce a pulse that comes to a steady-state amplitude equal to the cw amplitude. Consequently, there is an inequivalence uncertainty associated with any cw-to-pulse comparison.

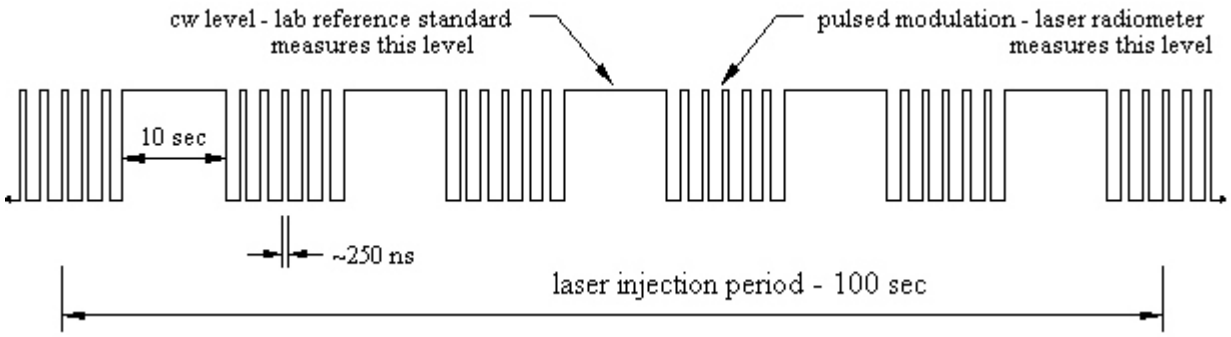

Figure 7. Sequence of a modulated laser signal for measurement of peak power (not to scale).

During the course of a measurement run, the low-level calibration system performs this comparison by alternating the laser modulation between cw and pulsed operation as shown in Figure 7. The fast-responding radiometer measures the pulsed signal, while the much slower laboratory standard measures only the cw portion of the laser beam. Calculations from the measured pulse characteristics and the total energy recorded by the lab standard are correlated using the beamsplitter ratio. The total injected energy measured by TC-24 yields the average peak power of the laser signal by the following calculation:

$$APP = \frac{MR - B}{TC \times CWT}, \tag{3}$$

where: APP = average peak power
MR = laboratory-standard reading
B = average baseline reading by laboratory standard
TC = laboratory-standard-traceable calibration factor (meter reading/J)
CWT = total time the laser signal is in cw mode

For laser pulses (Figure 8) with durations of 200 to 500 ns and a repetition rate of 500 Hz, the pulse characteristics have a very low duty-cycle and the picojoule energy levels are in the baseline noise of laboratory standard TC-24. However, a fast-responding semiconductor detector can follow the intensity profile of the pulse-modulated signal, and the peak voltage is recorded using an oscilloscope. The radiometer calibration factor is then calculated by the following equation:

$$K_{pp} = \frac{PV}{\left(APP/BSR\right)}, \tag{4}$$

where: K_{pp} = peak-power calibration factor (V/W)
PV = average peak voltage from the IUT (V)
APP = average peak power (W)
BSR = beamsplitter ratio (A/B ratio from Table 3.2)

Many users require that the input aperture of the radiometer be overfilled with a large, uniform beam. For this case, the aperture dimensions have been measured with an optical comparator, and the resulting area is used to calculate a responsivity factor in terms of unit area (V-cm^2/W):

$$\text{Responsivity} = \frac{PV}{\left(IP/A\right)}, \tag{5}$$

where IP equals the laser power incident on the radiometer, A is the aperture area of the instrument, and PV is the average peak voltage. Calibration factors for underfilled and overfilled input apertures are included with the calibration report for each laser radiometer.

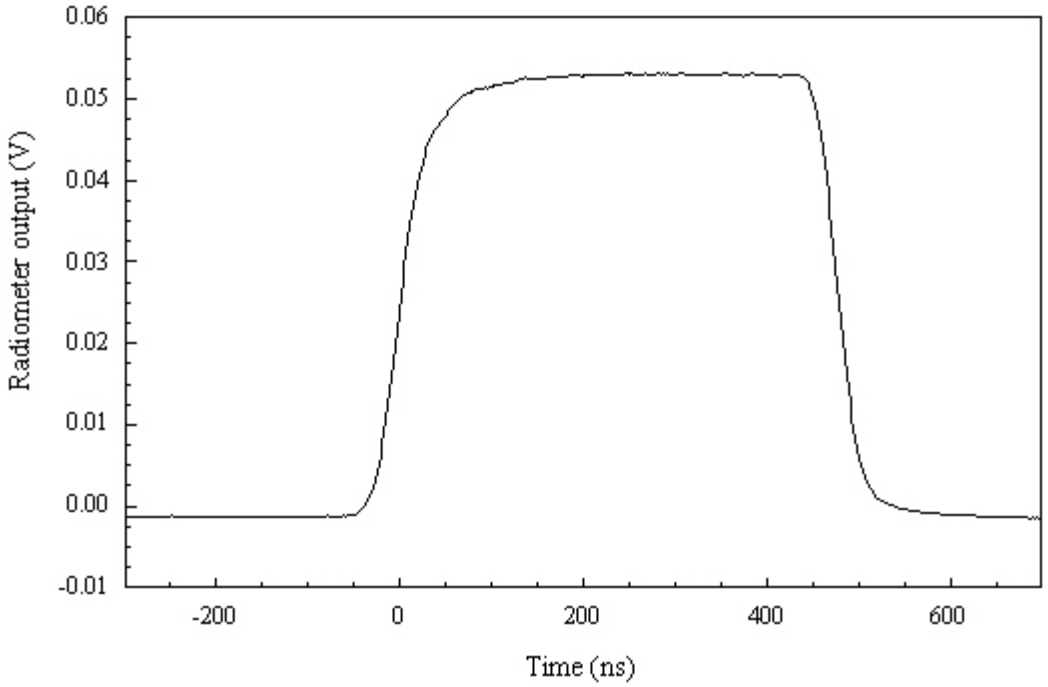

Figure 8. Typical waveform for peak-power calibration.

5.2 Bandwidth of Peak-Power Transfer Standards

For applications in laser measurement such as pulse energy or cw power, it is not necessary to know the impulse response of the detection system. However, in order to measure the shape or peak power of laser pulses, some knowledge of the impulse curve is required [1]. The output waveform of a laser radiometer is the convolution of the detection system's impulse response with the input laser pulse, and is described by the following equation:

$$V(t) = \int_{-\infty}^{+\infty} h(t') \cdot P(t - t')dt', \tag{6}$$

where *V(t)* is the voltage output of the detection instrument, *P(t)* is the input laser pulse, and *h(t)* is the impulse response of the detection instrument. By Fourier-transform theory, a fast impulse response in the time domain is equivalent to a wide bandwidth in the frequency domain.

Field transfer-standards for measuring peak power have been designed and constructed using APD detectors. Requirements for these instruments are high sensitivity along with a relatively wide bandwidth. Measurements of Gaussian pulses at a FDHM (Full-Duration Half-Maximum) from 10 to 30 ns are necessary for the calibration of laser guidance receivers (Section 1). This dictates a system bandwidth of 100 MHz or greater for accurate pulse reproduction. Practical constraints on the APD active area and sensitivity limit the bandwidth to about 50 MHz; as a result, the voltage output of the detector does not exactly match the laser pulse. The output of the radiometer is the convolution of the laser pulses with the detector's impulse response. Thus the impulse response of each APD detector must be measured to complete the calibration picture for a peak-power laser radiometer package.

6. MEASUREMENT OF DETECTOR IMPULSE RESPONSE

From linear systems theory, the electrical output of the APD is the convolution of the optical input pulse with the detector's impulse-response characteristics. This is important when the bandwidth of the detector is not much greater than the laser pulse. Currently available peak-power radiometers do not quite have the necessary bandwidth to replicate a 20 ns laser pulse to the desired accuracy, thus the motivation for this measurement. In order to rectify this deficiency, the impulse response of the APD detector is measured to quantify what effect limited bandwidth has on pulse fidelity.

6.1 Impulse Laser

The impulse response of the APD detector is tested by stimulating it with a pulsed-laser source that has a much shorter pulse duration (approximately 10 times shorter) than the expected response time of the detector. For our testing we used a 1.06 μm laser diode that has a FDHM of approximately 150 ps as measured by an even faster system.

6.2 Measurement of Detector Impulse Response

The impulse response waveform is obtained by measuring the response of the APD detector to the short laser pulse using a simple configuration as shown in Figure 9. A digital sampling oscilloscope (bandwidth: 1 GHz, risetime: 0.35 ns) is used to acquire the electrical output data.

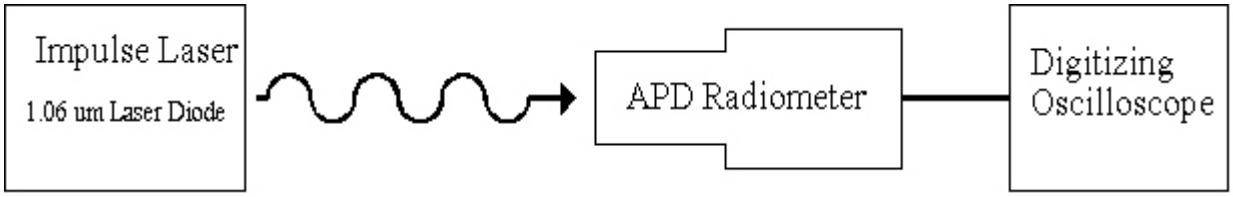

Figure 9. Configuration for measurement of impulse response.

A typical impulse waveform is shown in Figure 10. Overshoot, or ringing in the waveform, is due to the limited bandwidth of the APD. The digitized record of the waveform is saved on a floppy disk and transferred to a computer for signal processing.

Impulse-response waveforms are taken under varying conditions of signal intensity and optical alignment. These waveforms are normalized and numerically convolved with Gaussian-shaped pulses of various durations to estimate the effects of the limited bandwidth. This information is used to calculate correction factors that apply to the measured pulse peak and pulse duration. In these calculations, the FDHM range is from 10 to 30 ns since this is the region of interest. The waveforms are Gaussian to simulate the shape of the laser pulses in the equipment to be calibrated.

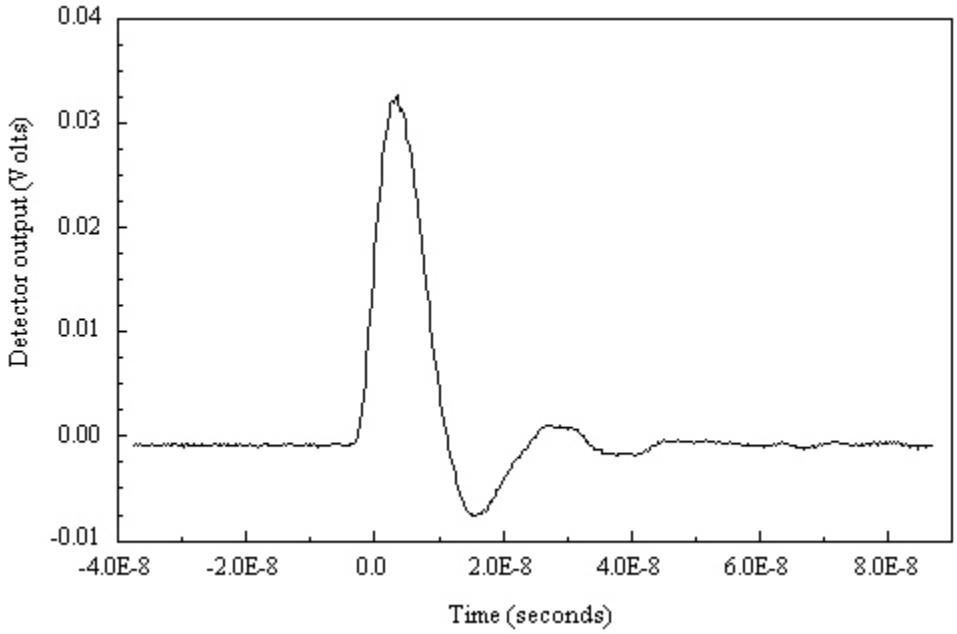

Figure 10. Typical impulse response waveform of APD radiometer.

A peak-power laser radiometer typically includes an external amplifier that can be switched into the circuit to provide additional gain for the lowest-level signals. Even though the amplifier we use is much faster than the APD detector and the expected laser pulses, its bandwidth still may affect the radiometer calibration factor. So the impulse response of the detector and amplifier together as a system is measured. Table 6.1 contains examples of typical correction factors to apply to measurements of peak voltage and pulse duration (see Appendix C).

Table 6.1. Sample bandwidth correction factors for APD 900-01.

Observed pulse duration, FDHM (ns)	Multiply peak voltage by:	Multiply pulse duration by:
10	1.28	0.72
11	1.17	0.80
12	1.11	0.86
13	1.07	0.90
14	1.05	0.92
15	1.04	0.95
16	1.03	0.96
17	1.02	0.97
18	1.02	0.98
19	1.01	0.99
20	1.01	0.99
21	1.01	1.00
22	1.01	1.00
23	1.01	1.00
24	1.01	1.00
25	1.01	1.00
26	1.01	1.01
27	1.01	1.01
28	1.01	1.01
29	1.01	1.01
30	1.01	1.00

7. MEASUREMENT UNCERTAINTY

The total uncertainty associated with a particular measurement of laser-pulse energy or peak power is composed of the individual uncertainties of the components of the entire system. The actual magnitude of the error of each uncertainty component is unknown; otherwise the result could be adjusted to eliminate the error.

Uncertainty estimates for our laser measurements are assessed using the following guidelines [6][7][8]. To establish the uncertainty limits, the sources of error are separated into Type A and Type B components. Components of uncertainty that are evaluated by statistical methods are called Type A uncertainty. Components of uncertainty that are evaluated by other means are designated as Type B uncertainty.

$$S_r = \sqrt{\frac{\sum_i (x_i - \bar{x})^2}{N-1}} \quad , \tag{7}$$

Type A uncertainties are assumed to be independent. The standard deviation S_r for each component iswhere the x_i values represent the individual measurements, $\bar{x}$ is the mean of the measurements, and N is the number of x_i values used for a particular component of Type A uncertainty. The standard deviation of the mean is $S_r/N^{1/2}$, and the total standard deviation of the mean is $[\Sigma_j(S_r^2/N)]^{1/2}$, where the summation is carried out for all the (j) uncertainty components of Type A.

The evaluation of Type B standard uncertainty is derived from scientific judgement based on previous measurement data, manufacturer's specifications, or any other relevant knowledge. For the low-level calibration system, all Type B uncertainties are assumed to be independent and to have rectangular or uniform distributions (that is, each error has an uniform probability of being within the region $\pm\delta_j$ and zero probability of being outside that region). If the distribution is rectangular, the standard deviation σ_s of each uncertainty component is equal to $\delta_j/3^{1/2}$, and the total standard deviation is $(\Sigma\sigma_s^2)^{1/2}$, where the summation is performed over all uncertainty components of Type B.

The expanded uncertainty is determined by combining the Type A standard deviation of the mean with the Type B standard deviation in quadrature and multiplying this result by a coverage factor of $k = 2$. This specifies an interval having a confidence of approximately 95 %. The expanded uncertainty U is then defined as

$$U = 2\sqrt{\sum \sigma_s^2 + \sum \frac{S_r^2}{N}} \quad . \tag{8}$$

The number of decimal places used in reporting the mean value of the measurements is determined by expressing the expanded uncertainty (in percentage) to two significant digits.

7.1 Uncertainty in the Laboratory Reference Standard

The reference standard used in the low-level calibration system is itself calibrated against a NIST primary standard. Individual components of uncertainty of this traceable calibration are included in the assessment of overall uncertainty of the low-level laboratory. Components of the uncertainty due to the calibration of the laboratory reference standard and its traceability to the C-series primary standard are documented in detail in other publications [9][10], and are briefly summarized as follows:

Type A uncertainty components for calibration of the reference standard in the C-series lab are:

(1) Electrical Calibration: The C-series calorimeters are calibrated by performing a large number of electrical measurements. The standard deviation of these calibration factors is approximately 0.1%.

(2) Sapphire Beamsplitter Calibration: Measurements of the beamsplitter ratios for the C-series lab are made periodically using the C-series calorimeters and a laser source. The standard deviation in these measurements is typically less than 0.2 %.

Type B uncertainty components for calibration of the reference standard in the C-series lab are:

(1) C-series Calorimeter Inequivalence: This component represents the uncertainty in measurements using the C-series calorimeters due to the difference between electrical and laser heating of the absorber cavity. Tests have shown this to be approximately 0.15 %.

(2) Absorptivity: A very small portion of the laser input will be reflected or scattered out of the absorber cavity and is not measured. The magnitude is less than 0.01 %.

(3) Heater Leads: Electrical current in the lead wires will produce heat that is not absorbed by the cavity and gives rise to a small error. This uncertainty is estimated to be less than 0.01 %.

(4) Electronics: Uncertainties in the various electrical measurements of the C-series calibration system are estimated to be less than 0.1 %.

(5) Sapphire Beamsplitter: Type B uncertainty for the sapphire beamsplitter ratios is estimated to be 0.2 %.

(6) Window Transmittance: Uncertainty in the measurements of the window transmittance of the C-series calorimeters is 0.16 %.

7.2 Pulsed-Laser Low-Level Measurement System Uncertainty

The total uncertainty for a calibration must also include sources of uncertainty from the low-level measurement system. The following components were evaluated to determine the magnitude of the contribution by the measurement system.

The Type A uncertainty components, which are evaluated by statistical methods are the following:

(1) Laboratory Reference-Standard, TC-24: The standard deviation in the measurement runs for calibrating reference-standard TC-24 with the C-series calorimeters is typically less than 0.6 %. This is the calibration data that provides traceability to the C-series primary standards. The laboratory reference-standard is calibrated every 12 to 18 months. The consistency of TC-24 as a reference standard is covered in detail in Section 8.1.

(2) Instrument Under Test: This uncertainty component is the standard deviation of the calibration runs performed by the low-level system on the IUT, or pulsed-laser radiometer. This data is specific to each calibration and for each radiometer. The magnitude depends on the instrument and conditions of measurement, and is typically 1 to 4 %.

Contributions of uncertainty evaluated by Type B methods are the following components:

(1) TC-24 Non-Uniformity: Non-uniformity in the absorber surface of the laboratory reference-standard will cause some uncertainty since the laser beam will not be incident upon exactly the same spot each time the system is aligned. The absorber surface is a polished glass plate with a 1° wedge, and the non-uniformity is estimated to be less than 1 %.

(2) Fused-Silica Beamsplitter: A beamsplitter ratio is used in all calibration measurements to calculate the energy or power incident on a test meter. The theoretical ratios (Table 3.1) are used because of the difficulty of directly measuring such large ratios and low power to a high accuracy. Accordingly, laser beamsplitter measurements are conducted only to confirm the theoretical ratios.

Measurements using a 1.06 μm source laser have confirmed the high-attenuation beamsplitter ratios to an uncertainty level of 2.1 %. This subject is covered in more detail in Section 8.2, and is part of the ongoing effort to reduce uncertainty values.

(3) Digitizing Oscilloscope: Measurements of the peak-to-peak voltage of the instrument under test are performed with a digitizing oscilloscope. This voltage waveform is correlated to the laser pulse characteristics of pulse energy or peak power. Performance specifications of the oscilloscope manufacturer for Δvoltage accuracy, gain error, and the estimated quantization error are combined in quadrature to provide an uncertainty estimate of 2 %.

(4) Leakage Effect: A small amount of cw laser power leaks through the modulator (A-O or E-O) even when the control signal is in the off state. A pulsed-laser radiometer will not respond to this cw signal; however, the reference-standard will detect the excess power, and the amount of laser energy registered will be in error. At lower levels, this leakage power is a greater fraction of the reference-standard measurement.

To compensate for this error, a baseline measurement is used to determine the amount of leakage for each specific configuration. Baseline measurements are made before and after each calibration run, and the average is subtracted from the reading obtained during the measurement run. Each baseline measurement is made with the shutter open, and the modulator transmission in the off state. The dual

baseline evaluations also provide correction for thermal drift in TC-24, which may occur during the calibration period. Measurements made to characterize the possible leakage effect after subtracting the baseline show a typical uncertainty of less than 0.7 % at the lowest power levels.

(5) Timing: Calibration-system timing issues contribute to the uncertainty associated with each of the low-level measurements. For pulse-energy calibrations, the timing uncertainty consists of the injection period, which is used to calculate the total energy absorbed by TC-24, and the uncertainty in the pulse repetition rate. Direct measurements of the shutter open/close period show an uncertainty of less than 0.1 %. Measurements on the instability of the pulse generator show an uncertainty in repetition rate of less than 0.3 %.

For peak-power calibrations, the uncertainty of the total time period during which the laser signal is in a cw mode determines the timing uncertainty factor. The total cw period is used to calculate the average peak-power from the energy measured by TC-24. This period is controlled by a precision timing generator and has a measured uncertainty of less than 0.6 %.

(6) Laser Stability: Laser pulse stability will directly impact the calibration measurements of peak power and pulse energy. However, any pulse-to-pulse instability is moderated by averaging many pulses during a simultaneous measurement with the reference standard and the IUT for pulse-energy calibrations. Measurements of the pulsed-laser signal have shown the instability of the averaged signal to be less than 0.8 % when using the acousto-optic modulator.

For peak-power, the laser signal is alternated between pulsed and cw, so the stability during the cw portion will affect the correlation measurement. Data for the cw-power stability show an uncertainty magnitude of 1 % or less.

(7) CW/Pulse Inequivalence: For peak-power calibrations the equivalence between the pulse power peak-level and the cw-level is the basis for correlating the measurement to a traceable standard. Ideally the laser pulse would attain the same level as the cw laser signal. Comparisons of these levels typically show a difference of less than 2.5 %. Careful alignment of the modulator and measurement checks with a dc-coupled detector fast enough to follow the pulse can reduce this to less than 1.5 %. Optical misalignment, laser pointing stability, and laser heating of the modulator influence this value to shift in an undetermined manner.

Energy calibrations have their own version of inequivalence since the modulated laser-pulse changes shape depending on the pulse duration of the input signal. If the modulator is driven near its risetime limit, then the edges of the pulse are rounded, producing a Gaussian-like shape. A flat-topped pulse is produced when the modulator is operated with pulse durations greater than three to four times longer than its risetime limit. The different pulse durations are necessary to provide sufficient energy to the laboratory reference standard, depending on the calibration parameters required by the customer.

The varying pulse shapes have an effect on the integrating amplifier of the pulse-energy radiometers. Calibrations of radiometer response using comparable laser pulse-energy but different pulse shapes (Figure 11) indicate a uncertainty of less than 2.5 %.

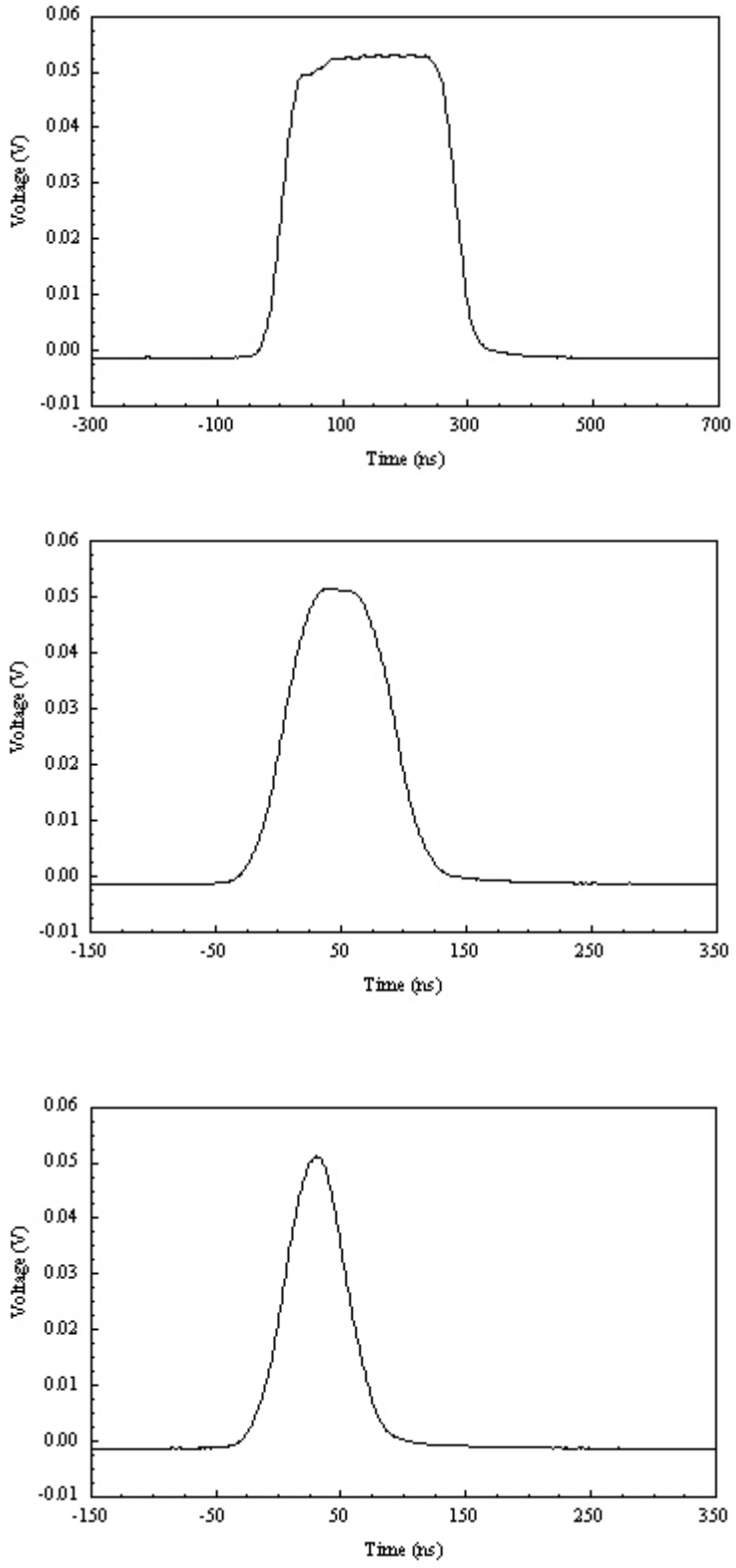

Figure 11. Input pulse shapes used to test inequivalence of pulse-energy radiometers.

7.3 Pulsed-Laser Radiometer Uncertainty Components

Characteristics of the laser radiometer or IUT also contribute to the overall uncertainty of its calibration factor. Normally NIST would not characterize specifications of the instrument to be calibrated, but all of the pulsed-laser radiometers calibrated with the low-level system have either been designed or constructed by the Optoelectronics Division and the customers depend on us for assessment of these quantities.

The following specifications have been characterized for laser radiometers as Type B uncertainty components.

(1) Bandwidth Correction: This component arises from the calculations of pulse duration and peak-power correction factors. As discussed in Section 6, for each peak-power radiometer the detector's impulse response is convolved with Gaussian pulses to determine what effect the limited detector bandwidth has on the radiometer response. The tests are done under a variety of conditions and signal levels with a typical standard deviation in the calculations of less than 1 %. Since we have a fairly short history of this measurement on any particular radiometer, we have included this uncertainty in the Type B components at a level of 1 %. This value will be re-evaluated as we obtain a larger body of measurements.

(2) Aperture Area: Typically the customer uses a laser radiometer with a large, uniform beam that overfills the input aperture. We do not have the equipment at NIST to perform measurements this way, so the calibrations are made with an underfilled beam. Measurements of the aperture dimensions are used to calculate an area, and a resulting calibration factor in terms of centimeter^2. The area uncertainty varies from 0.5 to 1.5 % depending on the aperture size and construction.

(3) Detector Nonuniformity: Since the laser spot will not be aligned exactly in the same place, then variations in the responsivity over the active area of the photodetector will add uncertainty to the calibration factor. Each radiometer is evaluated for these variations by manually scanning the laser beam over the detector surface and monitoring the voltage output. Pulse-energy instruments that use PIN detectors have variations on the order of 1 to 2 %, while APD-based radiometers have nonuniformity of 2 to 5 %.

(4) Temperature Stability: The responsivity of semiconductor detectors is temperature-sensitive. In order to stabilize the response under varying environmental conditions, temperature-control circuitry has been included in both the peak-power and pulse-energy radiometers. This control system functions by heating the detector module above ambient room temperature and holding it stable to ±1°C. The temperature-dependent responsivity of the APD detector module was measured as 0.2 %/°C, yielding an uncertainty magnitude of 0.2 %.

8. MEASUREMENT ASSURANCE

Historically, the expanded uncertainties for low-level laser radiometers have been fairly high, in the 8 to 12 % range. This is because of the relatively long traceablity chain, complex optical alignment, and high attenuation ratios necessary to realize low-level calibrations. Improvements to the measurement system and refining the assessment of uncertainty components have lowered the expanded uncertainty range to approximately 6 to 8 %, with an ultimate goal of 5 %.

Confidence in the accuracy, precision, and long-term stability of the low-level calibration system comes from the calibration histories of the laboratory reference standard and check standards.

8.1 Calibration History of the Laboratory Reference Standard

Laboratory reference standard TC-24 has been very stable over its calibration interval, as shown in Tables 8.1 and 8.2. The only significant change was a small shift in the calibration factor (reading/joule) when a failing display was replaced in April 1995.

As expected, changing the voltmeter/display for the TC-24 reference-standard yielded slightly different calibration factors as shown by comparing Table 8.1 to Table 8.2. All calibrations have their traceablity to the C-series primary standards.

Table 8.1 Early calibration history of TC-24.

Date	Range (joules)	Primary standard	Average power (mW)	Calibration factor (reading/J)	Expanded uncertainty (%)
4/27/88	unknown	Q-series	unknown	1.719	unknown
8/15/89	1	C-series	5.7	1.712	0.90
”	10	”	45	1.715	0.90
3/90	1	”	2-5	1.698	1.24
”	10	”	22-65	1.722	1.22
5/12/92	1	”	1	1.722	0.99
”	1	”	3	1.713	0.94
”	1	”	5	1.713	0.90
”	10	”	11	1.695	0.91
”	10	”	30	1.715	1.03
”	10	”	60	1.713	1.03

Table 8.2 Current calibration history for TC-24.

Date	Range (joules)	Primary standard	Average power (mW)	Calibration factor (reading/J)	Expanded uncertainty (%)
4/24/95	10	C-series	10	1.640	0.90
”	10	”	20	1.637	0.91
”	10	”	30	1.640	0.91
”	10	”	55	1.639	0.95
4/25/95	1	”	10	1.636	0.91
4/26/95	1	”	2.5	1.637	0.92
”	1	”	5	1.635	0.91
6/7/96	10	”	14	1.631	1.00
6/12/96	1	”	5	1.656	0.91
1/26/98	1	”	10	1.626	0.91
1/26/98	10	”	19	1.634	0.89
8/24/99	1	”	3.5	1.631	0.92
8/24/99	10	”	13	1.637	0.97
3/2001	1	”	4.6	1.620	1.00
3/2001	10	”	32	1.620	0.99

The data in these tables confirm the stability of the laboratory reference-standard TC-24, and the consistency of the calibration traceability to the C-series primary standards. From Table 8.2, the average calibration factor for TC-24 is 1.635 reading/joule with a standard deviation of 0.54 %.

8.2 Laser Beamsplitter Ratio Measurements

Measurements of the beamsplitter using a 1.06 μm source laser, germanium photodetectors, and a current meter showed results within 1.1 % of theoretical (Table 3.1) for the high order ratios. The low-order ratios have been confirmed to within 1.3 % in the C-series laboratory. The combined uncertainty estimate for the beamsplitter ratio is 2.1 %. Improvements to photodetectors and measurement techniques are being considered in an effort to reduce the uncertainty value further.

Much better results were achieved in the Laser Optimized Cryogenic Radiometer (LOCR) laboratory, where the source is a stabilized 1.550 μm laser. The beam is polarized and the quality is improved

with spatial filtering. Germanium trap detectors were used to measure the attenuation ratios. The LOCR facility is a high-accuracy laser power standard operated by the Optoelectronics Division [11]. At 1.550 μm there was less than 1 % difference between the theoretical and measured ratios for a fused-silica beamsplitter, including the higher orders. While the specific wavelength of interest was not demonstrated, we believe that it can be, once a similar measurement can be set up at 1.06 μm. Until this can be completed, the higher uncertainty magnitude of 2.1 % is used for calibration purposes.

8.3 Using the Calibration History of Check Standards to Monitor the Low-Level System

Confidence in the long-term stability in the 1.06 μm low-level calibration system is supported from calibration histories of the original laser radiometers built at NIST. Due to the time and expense necessary to construct and calibrate these instruments, a single radiometer has not been reserved for NIST use as a check standard. However, a substantial calibration history exists for several pulse-energy and peak-power radiometers.

8.3.1 Check Standards for Pulse-Energy Calibrations

Two pulse-energy radiometers for which we have a long-term calibration history have been operated by NIST as Measurement Assurance Program (MAP) standards. The calibration factor for only the ×10 amplifier gain for each radiometer are shown in Table 8.3.

Table 8.3 Pulse-energy calibration history, amplifier gain = 10

Date	Radiometer	Nominal pulse energy (J)	Calibration factor (J/V)	Number of runs	Standard deviation (%)	Expanded uncertainty (%)
1989-98	PIN 4-1	2×10^{-13}	2.29×10^{-13}	36	1.66	6.5
1990-98	PIN 4-3	5×10^{-13}	2.45×10^{-13}	51	1.59	6.5

While these instruments have been calibrated infrequently, the calibration factor consistency is good for this type of measurement, with a standard deviation of less than 2 %. The expanded uncertainty for the calibration factor for each radiometer is 6.5 %.

8.3.2 Check Standards for Peak-Power Calibrations

Three peak-power radiometers have significant calibration history with the low-level measurement system. Instruments APD-721 and APD-723 were designed and built at NIST, but are owned and operated by the U.S. Air Force. The units are shipped to NIST for calibration every 1 to 2 years, so there is a significant history and consistent operation. An identical radiometer, APD-725, is calibrated and operated by NIST as a MAP standard. It has been used off-site by various customers, but has a meaningful calibration history as well. Tables 8.4 to 8.6 summarize the calibration factors for each peak-power radiometer configured with no external amplifiers.

Table 8.4 APD-721 peak-power calibration history.

Date	Amplifier gain (dB)	Nominal peak-power (μW)	Calibration factor [V/(W/cm^2)]	Number of runs	Standard deviation (%)	Expanded uncertainty (%)
4-90	0	2	1.77×10^4	13	2.72	6.98
7-92	0	2	1.79×10^4	16	3.28	6.97
4-94	0	0.1-20	1.88×10^4	30	2.38	7.01
5-95	0	0.2-20	1.89×10^4	12	1.27	7.30
3-97	0	0.2-14	1.87×10^4	20	1.23	7.10
4-98	0	0.8-25	1.89×10^4	16	1.68	6.92
1-00	0	0.5-25	1.83×10^4	27	2.67	7.98

The standard deviation of the mean of the calibration factors for APD-721 and 723 are respectively 2.7 % and 2.1 %. This gives us an estimate of the peak-power measurement consistency of the low-level calibration system.

Table 8.5 APD-723 peak-power calibration history.

Date	Amplifier gain (dB)	Nominal peak-power (μW)	Calibration factor [V/(W/cm^2)]	Number of runs	Standard deviation (%)	Expanded uncertainty (%)
11-91	0	2	1.78×10^4	15	2.72	7.31
6-93	0	2	1.74×10^4	14	2.26	7.27
2-95	0	0.2-20	1.74×10^4	12	2.08	6.77
4-96	0	0.1-25	1.80×10^4	32	5.13	6.93
1-98	0	2-25	1.80×10^4	16	4.56	6.98
1-99	0	0.5-25	1.71×10^4	16	1.53	6.89
1-00	0	0.5-25	1.73×10^4	26	1.45	7.07
1-01	0	0.5-20	1.72×10^4	20	1.78	7.09
1-02	0	0.6-21	1.72×10^4	26	0.72	7.10
3-03	0	1.2-21	1.70×10^4	21	1.71	6.90

Further confirmation of the consistency is shown in Table 8.6, the calibration history for APD-725. This unit has been sent several times to customer sites, and has been partially disassembled, which may affect the responsivity. It still maintains a standard deviation less than 2.4 % for its calibration factor.

Table 8.6 APD-725 peak-power calibration history

Date	Amplifier gain (dB)	Nominal peak-power (μW)	Calibration factor [V/(W/cm^2)]	Number of runs	Standard deviation (%)	Expanded uncertainty (%)
6-91	0	0.3-1	1.66×10^4	10	0.76	7.40
2-92	0	0.8-40	1.61×10^4	14	2.87	7.54
9-93	0	0.3-50	1.66×10^4	16	1.66	7.33
3-94	0	0.8-2.7	1.64×10^4	4	2.36	7.75
8-98	0	1-25	1.57×10^4	32	2.14	6.67

Calibration factors for both pulse-energy and peak-power radiometers have been fairly consistent and within the estimated uncertainty levels.

8.4 Revising the Uncertainty Levels from Accumulated Data

A substantial volume of data has been accumulated from radiometer calibrations, laboratory reference-standard calibrations, and beamsplitter ratio measurements. These records are the evidence for the long-term consistency of the low-level, 1.06 μm calibration system, and new measurements are combined with the previous data as part of the quality control.

The laboratory standard, beamsplitter ratios, digital oscilloscope, laser stability, and cw/pulse inequivalence are system uncertainty components that are most likely to change. They are evaluated annually and updated. Laser beamsplitter ratios and cw/pulse inequivalence are the uncertainty components that need the most attention and are two of the more difficult values to measure. These two components are also where the most reduction in uncertainty is feasible.

9. FUTURE CHANGES IN CALIBRATION SYSTEM

Inevitably, changes will be made to the 1.06 μm, low-level calibration system. A different laboratory reference standard is a possible development to decrease the measurement run time. Updates to measurement instrumentation will be considered to lower uncertainties. Software has been developed to control data acquisition, and to enhance measurement statistics.

The majority of modifications in the near future will probably be minor. Changes in documentation will be updated in a notebook kept with the system. While the details may no longer be completely accurate, this report should adequately describe the service.

Major changes such as a new laboratory reference standard, or different software control of the measurement system, will require the documentation to be updated.

10. REFERENCES

[1] Saunders, A.A.; Rasmussen, A.L.; A System for Measuring Energy and Peak Power of Low-Level 1.064 μm Laser Pulses. *National Bureau of Standards (U.S.) Technical Note 1058*: 1982; 39p.

[2] Beers, Y.; The Theory of the Optical Wedge Beam Splitter. *National Bureau of Standards (U.S.) Monograph 146*: 1974. 26p.

[3] Danielson, B.L.; Measurement Procedures for the Optical Beam Splitter Attenuation Device BA-1. *National Bureau of Standards (U.S.) Internal Report 77-858*: 1977. 20p.

[4] Malitson, I.H.; Interspecimen Comparison of the Refractive Index of Fused Silica. *Journal of the Optical Society of America* Vol. 55: 1205-1209; Oct. 1965.

[5] Edlin, Bengt; The Index of Refraction of Air. *Metrologia,* Vol. 2, No. 2; 1966; pp. 71-80.

[6] Taylor, B.N.; Kuyatt, C.E.; Guidelines for Evaluating and Expressing the Uncertainty of NIST Measurement Results. *National Institute of Standards and Technology Technical Note 1297*: 1994; 20p.

[7] Eisenhart, C.; Ku, H.H.; Colle', R.; Expression of Uncertainties of Final Measurement Results: Reprints. *National Bureau of Standards (U.S.) Special Publication 644*: 1983.

[8] Wagner, S.R.; On the Quantitative Characterization of the Uncertainty of Experimental Results in Metrology. PTB-Metteilungen 89: 1979; pp. 83-89.

[9] West, E.D.; Case, W.E.; Rasmussen, A. L.; Schmidt, L.B.; A Reference Calorimeter for Laser Energy Measurements. *Journal of Research of the National Bureau of Standards-A. Physics and Chemistry*, 76A, No.1: Jan-Feb 1972; pp. 13-26.

[10] West, E.D.; Case, W.E.; Current Status of NBS Low-Power Laser Energy Measurement. *IEEE Transactions on Instrumentation and Measurement* Vol IM-23, No.4: Dec. 1974, pp. 422-425.

[11] Livigni, D.J.; Cromer, C.L.; Scott, T.R.; Johnson, B.C.; Zhang, Z.M.; Thermal Characterization of a Cryogenic Radiometer and Comparison with a Laser Calorimeter. *Metrologia,* 35; 1998; pp. 819-827.

[12] Bracewell, R.N.; *The Fourier Transform and Its Applications*, second edition, McGraw-Hill, New York, 1978; p. 108-112.

Appendix A: Sample Calibration Report

U.S. DEPARTMENT OF COMMERCE
NATIONAL INSTITUTE OF STANDARDS AND TECHNOLOGY
ELECTRONICS AND ELECTRICAL ENGINEERING LABORATORY
Boulder, Colorado 80305

REPORT OF CALIBRATION

LOW-LEVEL TRANSFER STANDARD
National Institute of Standards and Technology
APD 900-01

Submitted by:
Customer's Name
Customer's Address

Measurement Summary

I. Peak Power Calibration

The low-level transfer standard APD 900-01 was calibrated for peak-power response against a NIST laboratory-standard traceable to the national standard calorimeters maintained by NIST. The comparison measurements between APD 900-01 and the NIST standard were performed using a cw Nd:YAG laser (wavelength = 1.06 μm) whose output was "chopped" into "flat-top" shaped pulses (<400 ns duration) with an acousto-optic modulator (see Figure 1). The "chopped" beam was then incident onto a multiple reflection, polished, fused silica, wedged beamsplitter, with the NIST standard placed in the main transmitted beam and APD 900-01 was placed in a lower power (higher order) beam.

The output of APD 900-01 was measured with a digital oscilloscope (50 Ω impedance) and the average **peak-to-peak** voltage reading was obtained. The calibration factor for APD 900-01 was determined by dividing the average voltage peak of its output by the average peak-power incident onto the transfer standard. Assuming the beam is smaller than the input aperture, when the output of the detector is **divided** by the appropriate calibration factor listed in Tables I or II, the resulting peak power will agree (on the average) with NIST standards.

Table I. Calibration Summary-Peak Power (small beam; no filters)

Amplifier Gain	Number of Measure-ments	Calibration Range for Peak-Power	Calibration Factor (V/W)	Standard Deviation	Expanded Uncertainty (k=2)
x1	16	0.1 - 7 μW	$9.92 \cdot 10^4$	1.64%	6.3%
x10	12	40 - 750 nW	$9.43 \cdot 10^5$	0.85%	6.3%

Page: 1 of 7
Date of Report: March 10, 1998
Test No.: xxxxxx

Table II. Calibration Summary (small beam with neutral density filter)					
Amplifier Gain & Filter Type	**Number of Measure-ments**	**Nominal Pulse Peak Power Range**	**Calibration Factor (V/W)**	**Standard Deviation**	**Expanded Uncertainty**
x1, Neutral Density	12	1 - 60 μW	$4.64 \cdot 10^3$	2.47 %	6.4%

If this radiometer is used to measure the radiation in a uniform irradiance beam which is larger than the input aperture, then the peak (with respect to time) power irradiance can be found using calibration factors from Table III. These factors were obtained by multiplying the factors in Tables I and II by the cross sectional area of each of the apertures. The uncertainties associated with the values in Table III must include the uncertainties listed in Tables I and II but in addition, the uncertainty due to non-uniformity properties of the laser beam must be added. NIST does not have the capability (i.e., large uniform laser beam) to further characterize measurement errors when using large beams with this instrument.

Table III. Calibration Factors for Use With Apertures (large beam)					
Gain	**Aperture 1 79.95 cm^2 area V/(W/cm^2)**	**Aperture 2 19.95 cm^2 area V/(W/cm^2)**	**Aperture 3 4.971 cm^2 area V/(W/cm^2)**	**Aperture 4 0.980 cm^2 area V/(W/cm^2)**	**ND Aperture 4.924 cm^2 area V/(W/cm^2)**
x1	$7.93 \cdot 10^6$	$1.98 \cdot 10^6$	$4.93 \cdot 10^5$	$9.73 \cdot 10^4$	$2.28 \cdot 10^4$
x10	$7.54 \cdot 10^7$	$1.88 \cdot 10^7$	$4.69 \cdot 10^6$	$9.24 \cdot 10^5$	--------

Bandwidth Correction Factors

Impulse response measurements performed on APD 900-01 (with and without the amplifier) indicate a risetime of approximately 5 ns; consequently, a correction must be made to its voltage output signal when using short (<50 ns) input pulses. To obtain the appropriate correction factors, the impulse response of APD 900-01 was convolved with Gaussian waveforms of various pulse durations ranging from 10 to 30 ns. Using the observed pulse duration as a guide, the appropriate correction factors should be multiplied times the pulse duration and peak voltage to obtain the estimated optical pulse duration and peak optical power.

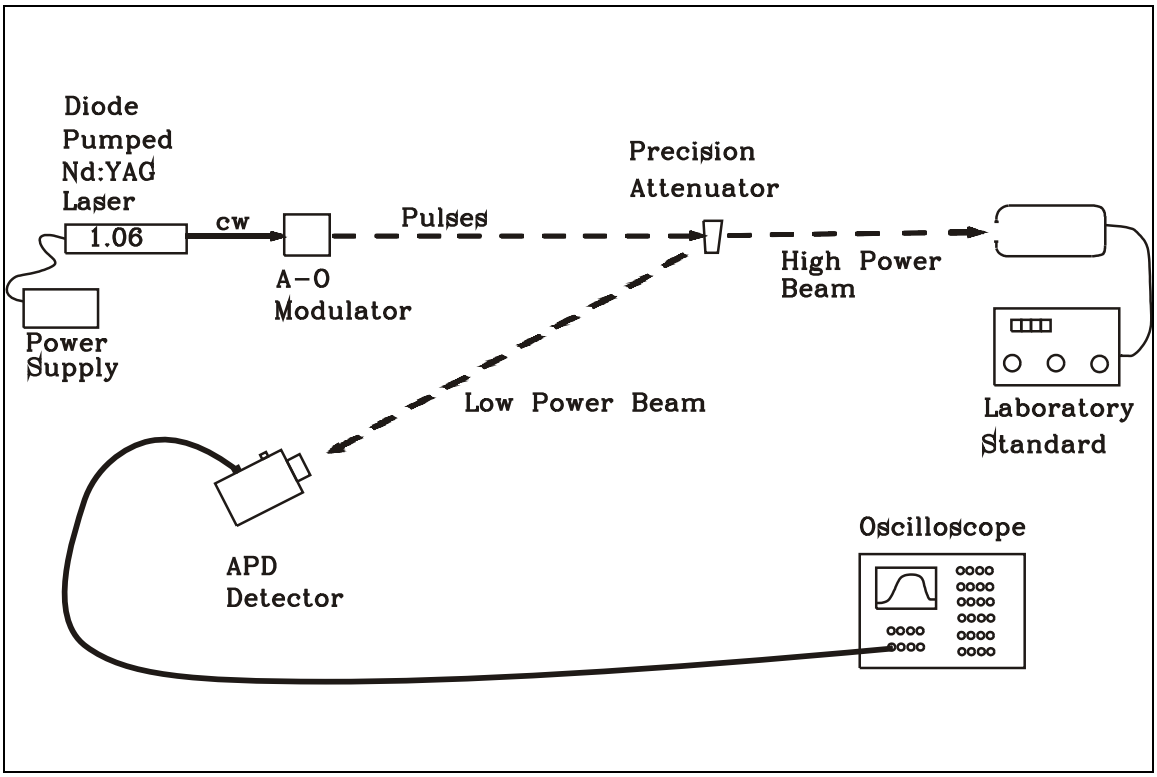

Figure 1. Low-level Pulsed-Laser Measurement Configuration.

Pulse Energy Calibration

The low-level transfer standard APD 900-01 was also calibrated for pulse-energy response against a NIST laboratory standard traceable to the national standard calorimeters maintained by NIST. The comparison measurements between APD 900-01 and the NIST standard were performed using a cw Nd:YAG laser (wavelength = 1.06 μm) whose output was "chopped" into "flat-top" shaped pulses (<200 ns duration) with an acousto-optic modulator (see Figure 1). The "chopped" beam was then incident onto a multiple reflection, polished, fused-silica beamsplitter where the NIST standard was placed in the main transmitted beam and APD 900-01 was placed in a lower energy (higher order) beam.

The output of APD 900-01 was measured with a digital oscilloscope (50 Ω impedance, dc coupled) and the average **peak-to-peak** voltage reading was obtained. The calibration factor for APD 900-01 was determined by dividing the average pulse energy incident onto the detector by the average voltage output of the radiometer. Assuming the beam is smaller than the input aperture, when the output of the detector is **multiplied** by the appropriate calibration factor listed in Tables IV or V, the resulting pulse energy will agree (on the average) with NIST standards.

Table IV. Calibration Summary - Pulse Energy (small beam; no filters)

Amplifier Gain	Number of Measure-ments	Nominal Pulse Energy Range	Calibration Factor (J/V)	Standard Deviation	Expanded Uncer-tainty
x10	12	0.1 - 2.3 pJ	$2.11 \cdot 10^{-12}$	1.07%	6.3%
x100	12	4 - 200 fJ	$2.08 \cdot 10^{-13}$	1.73%	6.3%

Table V. Calibration Summary (small beam with neutral density filter)

Amplifier Gain & Filter Type	Number of Measure-ments	Nominal Pulse Energy Range	Calibration Factor (J/V)	Standard Deviation	Expanded Uncer-tainty
x10 Neutral Density	12	0.8 - 50 pJ	$4.45 \cdot 10^{-11}$	3.15%	6.5%

If this radiometer is used to measure the radiation in a uniform irradiance beam which is larger than the input aperture, then the pulse radiant exposure can be found by using calibration factors from Table VI. These factors were obtained by dividing the factors in Tables IV and V by the cross sectional area of each of the apertures. The uncertainties associated with the values in Table VI must include the uncertainties listed in Tables IV and V but in addition, the uncertainty due to non-uniformity properties of the laser beam should be added. NIST does not have the capability (i.e., large uniform laser beam) to further characterize measurement errors when using large beams with this instrument.

Table VI. Calibration Factors for Use With Apertures (large beam)

Gain	Aperture 1 79.95 cm^2 area $(J/cm^2)/V$	Aperture 2 19.95 cm^2 area $(J/cm^2)/V$	Aperture 3 4.971 cm^2 area $(J/cm^2)/V$	Aperture 4 0.980 cm^2 area $(J/cm^2)/V$	ND Aperture 4.924 cm^2 $(J/cm^2)/V$
x10	$2.64 \cdot 10^{-14}$	$1.06 \cdot 10^{-13}$	$4.24 \cdot 10^{-13}$	$2.15 \cdot 10^{-12}$	$9.04 \cdot 10^{-12}$
x100	$2.60 \cdot 10^{-15}$	$1.04 \cdot 10^{-14}$	$4.18 \cdot 10^{-14}$	$2.12 \cdot 10^{-13}$	--------

Uncertainty Assessment

The uncertainty estimates for the NIST laser energy and peak-power measurements are expressed and combined using the following guidelines. To establish the uncertainty limits, the error sources are separated into (1) Type B errors whose magnitudes are determined by scientific judgement and (2) Type A magnitudes are obtained statistically from a series of measurements.

All the Type B components are assumed to be independent and have rectangular or uniform distributions (that is, each has an equal probability of being within the region, $\pm\delta_i$, and zero probability of being outside that region). If the distribution is rectangular, the standard deviation σ_s, for each Type B uncertainty component is equal to $\delta_i/3^{1/2}$ and the total "standard deviation" is $(\Sigma\sigma_s^2)^{1/2}$ where the summation is performed over all Type B components.

The Type A components are assumed to be independent and the standard deviation, S_r, for each component is:

$$S_r = \sqrt{\frac{\sum_i (x_i - \bar{x})^2}{N-1}} \quad , \qquad \textbf{(A1)}$$

where the x_i values represent the individual measurements and N is the number of x_i values used in measuring the quantity for a particular Type A uncertainty component. The standard deviation of the mean is $S_r/N^{1/2}$, and the total standard deviation of the mean is $[\Sigma_j(S_r^2/N)]^{1/2}$, where the summation is carried out for all the Type A components.

The total expanded uncertainty is determined by combining the Type A and Type B uncertainty estimates in quadrature and multiplying this result by a coverage factor of 2. The expanded uncertainty, U, is then

$$U = 2\sqrt{\sum \sigma_s^2 + \sum \frac{S_r^2}{N}} \quad . \qquad \textbf{(A2)}$$

The values used to calculate the expanded uncertainty are listed in Tables VII and VIII. The number of decimal places used in reporting the mean values of the calibration factors listed in Tables I and IV were determined by expressing the expanded uncertainty (in percentage) to two significant digits.

Table VII. Measurement Uncertainties for Peak-Power Calibration

TYPE B		TYPE A		
Source	σ_i	**Source**	S_r	**N**
Inequivalence	0.09%	Electrical Calibration	0.10%	30
Absorptivity	0.01%	Beamsplitter Calibration	0.08%	17
Heater Leads	0.01%	Trans Std (TC-24) Cal	0.54%	24
Electronics	0.06%	Trans Std (APD 900-01) Cal	See	Table I
Sapphire B/S	0.12%			
Window Transmittance	0.09%			
TC-24 Non-Uniformity	0.58%			
Fused Silica B/S	1.21%			
Scope (Digital)	1.15%			
Leakage Effect	0.40%			
Timing	0.35%			
CW/Pulse Inequiv.	1.44%			
Temp. Stability	0.58%			
Bandwidth Correction	0.58%			
Aperture Area	0.87%			
APD/Lens Non-Uniformity	1.44%			
Laser Stability	0.87%			

Table VIII. Measurement Uncertainties for Pulse Energy Calibration

TYPE B		TYPE A		
Source	σ_i	**Source**	S_r	**N**
Inequivalence	0.09%	Electrical Calibration	0.10%	30
Absorptivity	0.01%	Beamsplitter Calibration	0.08%	17
Heater Leads	0.01%	Trans Std (PIN 4-3) Cal	2.9%	12
Electronics	0.06%	Trans Std (APD 900-01) Cal	See	Table IV
Sapphire B/S	0.12%			
Window Transmittance	0.09%			
TS Non-Uniformity	0.58%			
Fused Silica B/S	1.21%			
Scope (Digital)	1.15%			
Leakage Effect	0.40%			
Timing	0.18%			
Pulse Inequivalence	1.44%			
Temperature Stability	0.58%			
Aperture Area	0.87%			
APD/Lens Non-Uniformity	1.44%			
Laser Stability	0.87%			

For the Director,
National Institute of Standards and Technology

Calibrated by,

Thomas R. Scott, Group Leader
Sources and Detectors Group
Optoelectronics Division

Rodney W. Leonhardt, Electronics Engineer
Sources and Detectors Group
Optoelectronics Division

Page: 7 of 7
Date of Report: March 10, 1998
Test No.: xxxxxx

APPENDIX B. Calibration Procedure Outline

1. Ascertain the laser radiometer's type and the desired calibration conditions from the customer.

2. From the low-level performance specifications, calculate whether the measurement system can be configured to meet the customer's requirements.

3. Check the system output for those requirements by using a cw power meter or the laboratory transfer-standard, TC-24 to measure the energy level.

4. If the power and/or energy levels and beam diameter can be adjusted to match the customer requirements, then the calibration can commence. At this point the customer should make arrangements for payment and shipping with the Optoelectronics Office of Measurement Services, NIST-Boulder, phone (303) 497-4285 or FAX 303-497-4286 or email: caliopto@boulder.nist.gov. The internet address for NIST technology services and general calibration information is http://ts.nist.gov/ts/

5. Once the test radiometer arrives, unpack and set up the equipment to be calibrated in the low-level enclosure. The customer should include all cables and connectors necessary to calibrate the instrument. If NIST provides cables, then the customer should be notified that these differing conditions may change the calibration factor. Allow the detector head and electronics to stabilize overnight at room temperature.

6. Turn on the low-level system laser and electronics; then the test instrument should be activated and allowed to warm up for at least one hour before calibration-quality measurements are made.

7. Check alignment of the laser beam through all optical components of the calibration system. This includes collimating lenses, polarizer, modulator, apertures, beamsplitter, and transfer standards. Carefully align the IUT in the appropriate beam. The beam incoming on the IUT should be reflected roughly back on itself. Maximize or "peak" the signal output from the test instrument.

8. Adjust system parameters such as peak-power level, pulse width, or pulse energy to match the required calibration conditions. Perform at least 8 to 12 calibration runs on the radiometer for each amplifier configuration. Vary the laser-pulse levels in order to test the radiometer's linearity and performance under different conditions.

9. Calculate the calibration factors and measurement uncertainty using NIST statistical guidelines [5]. Prepare calibration report and return equipment with original signed copy of the report to the Office of Measurement Services for shipment to the customer.

APPENDIX C. Impulse Response Measurement and Bandwidth Correction Calculation

C.1 The need for impulse response measurement of pulsed-laser detectors

We calibrate each photodiode-based peak-power transfer standard using long-duration laser pulses that essentially allow us to measure the steady-state responsivity of the detector. However, when these detectors with limited bandwidth are used to measure relatively short (<80 ns) laser pulses, the pulse characteristics (e.g., duration and peak value) of the output electrical response are distorted when compared to the input optical pulse. Accordingly, a measurement of the impulse response of the pulsed-laser radiometer is necessary to ascertain the effect the limited bandwidth will have on short-period signals (Section 5.2) and to correct for it. We do this with a simple correction factor as described below.

For linear systems, the output signal can be expressed mathematically as the convolution of the input signal with the impulse response of the system. Since the detector and oscilloscope are linear systems, we estimate a detector's behavior when measuring short optical-pulses, convolving its impulse response with simulated pulse waveforms having various pulse durations of interest.

To compute this convolution, we rely on the fact that the convolution of two functions is the inverse Fourier transform of the product of their Fourier transforms [12]. Thus, to estimate the behavior (and obtain the corresponding correction factors) of the photodiode detectors, we calculate the inverse Fourier transform of the product of the Fourier transforms of both the simulated input signal and the impulse response.

Knowing that the area under a convolution is equal to the product of the areas of the two curves being convolved [12], we can scale the convolution by dividing by the area under the impulse response curve. This scaling is done since we require that the pulse energy represented by the area under the curves to be the same for both the input and output signals (i.e., we are considering distortions to the pulses, not losses in the system). The correction factors are then found by taking the ratio of the peak (FDHM) of the input Gaussian waveform to the peak (FDHM) of the convolved waveform, scaled as described above. Example correction factors are given in Table 6.1.

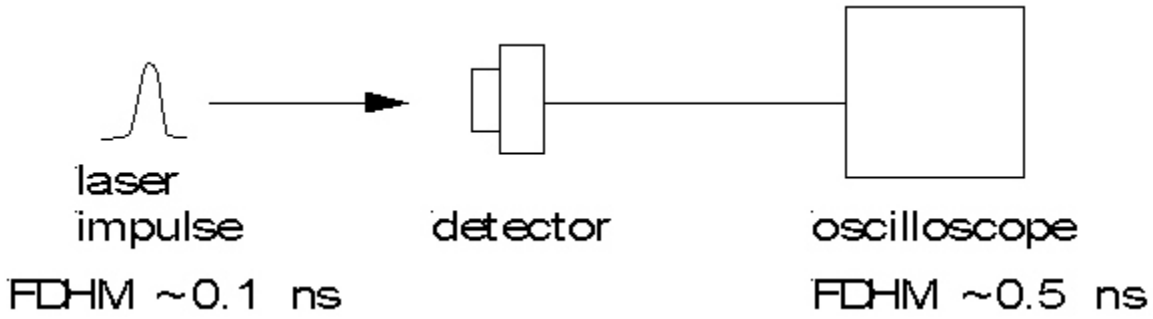

Figure C1. Measurement configuration for impulse response.

C.2 Bandwidth correction procedure

1. Measure detector impulse response with configuration shown in Figure C1. The impulse response curves are acquired by recording the voltage signal from the detector in response to very short laser pulses incident on the detection instrument. Typically the input pulses are about 120 ps in duration, which is about 1/40 the impulse response of the detector.

   The configuration (Figure C1) will measure the impulse response of the detector, cable, oscilloscope as a unit. The relatively slow detector (~5 ns risetime) will dominate the impulse waveform. As a result, the wideband (1 GHz bandwidth, 0.4 ns risetime) oscilloscope does not contribute significantly to the impulse response measurement.

2. Generate the simulated input laser-pulse waveforms. These are simulated pulses which have Gaussian shapes of various pulse durations covering the time region of interest. The pulse durations range from 10 to 30 ns (FDHM), using 1 ns increments.

3. Fourier transforms of the impulse response and the generated (Gaussian) waveforms are calculated separately.

4. Inverse Fourier transform of the product of the two transforms in step 3 is calculated.

5. The result is divided by the area under the detector impulse-response curve.

6. The resulting peaks and durations of the convolutions are compared to those of the input waveforms, to determine the correction factors for each pulse duration.

7. The correction factors are tabulated and graphed according to the observed pulse duration. One factor is to restore the peak voltage reading and the other is to correct the pulse duration.

The correction factors have been calculated using two different software packages and approaches. One technique was to use the Fourier-transform method described above and was implemented with a Fast Fourier Transform (FFT) using two different high-level mathematical programs. The other method carried out the convolutions directly in the time domain by performing the numerical integration using one of the mathematical programs. The results agreed, and currently the Fourier-transform method is used because it is less computationally intensive and thus much faster.

Impulse-response data are taken for each gain setting, and under different signal levels, to test the entire range of conditions in which the radiometer may be used (i.e., to test the radiometer's linearity). The resulting correction factors typically show a standard deviation of about 1 %. A typical sample of the correction factors for an APD radiometer is shown in Table 6.1.

APPENDIX D: Suitable Transfer Standards and Shipping Instructions

D.1. Transfer standards that are suitable for calibration

The transfer standards that are suitable for calibration in the low-level 1.06 μm system must be able to measure pulsed laser energy within the range of 100 fJ to 10 nJ or peak power from 40 nW to 5 mW. The transfer standard should also operate with laser pulse durations within the range of 20 ns to 2 μs (FDHM). The transfer standard must convert the laser pulse to a voltage waveform with an output impedance of 50 Ω or 1 MΩ for measurement with an oscilloscope. The peak voltage of the waveform should be in the range of 10 mV to 5 V.

An output cable with a BNC connector for matching to a standard oscilloscope input should be provided by the customer, as the NIST calibration factors will include the cable in the configuration. We recommend the end user of the transfer standard have an oscilloscope that has a minimum bandwidth of 350 MHz, although ≥500 MHz is preferable for peak-power measurements.

D.2. Shipping instructions for transfer standards

Transfer standard equipment should be shipped in well-padded foam, or otherwise mechanical-shock insulated cases, appropriate for reshipment back to the customer. Equipment within the case should not be allowed to move around or else should be appropriately insulated. Operation instructions or instruction manuals should be included, as well as customer-chosen set-up parameters for instrument functions, including bias voltage, and amplifier gains to be calibrated. The customer should include all cables and connectors that are necessary to calibrate the transfer standard as specified.